In this study, we examined classification using only three types of movements and one type of feature. We feel that our results suggest the need to evaluate neurological profiles of participants before the application of invasive clinical BMI techniques, and that this may be valid even when using other movement types and features. However, as there have been few reports in terms of this, further studies are needed in order to clarify the generality of our results.

Conclusion

Decoding accuracies at the latencies of three MRCF components largely exceeded the chance level in all participants. The amplitude of neurophysiological responses reflected decoding accuracies. We propose that BMI performance can be predicted by evaluating neurophysiological profiles.

Acknowledgements

This work was supported by a grant to T. Yoshimine and M. Hirata for 'Brain Machine Interface Development' from the Strategic Research Program for Brain Sciences funded by the Ministry of Education, Culture, Sports, Science, and Technology of Japan.

Conflicts of interest

There are no conflicts of interest.

References

1 Hochberg LR, Serruya MD, Friehs GM, Mukand JA, Saleh M, Caplan AH, *et al.* Neuronal ensemble control of prosthetic devices by a human with tetraplegia. *Nature* 2006; **442**:164–171.
2 Wolpaw JR, McFarland DJ. Control of a two-dimensional movement signal by a noninvasive brain-computer interface in humans. *Proc Natl Acad Sci USA* 2004; **101**:17849–17854.
3 Nijboer F, Sellers EW, Mellinger J, Jordan MA, Matuz T, Furdea A, *et al.* A P300-based brain-computer interface for people with amyotrophic lateral sclerosis. *Clin Neurophysiol* 2008; **119**:1909–1916.
4 Velliste M, Perel S, Spalding MC, Whitford AS, Schwartz AB. Cortical control of a prosthetic arm for self-feeding. *Nature* 2008; **453**:1098–1101.
5 Rickert J, Oliveira SC, Vaadia E, Aertsen A, Rotter S, Mehring C. Encoding of movement direction in different frequency ranges of motor cortical local field potentials. *J Neurosci* 2005; **25**:8815–8824.
6 Mehring C, Rickert J, Vaadia E, Cardosa de Oliveira S, Aertsen A, Rotter S. Inference of hand movements from local field potentials in monkey motor cortex. *Nat Neurosci* 2003; **6**:1253–1254.
7 Lotte F, Congedo M, Lecuyer A, Lamarche F, Arnaldi B. A review of classification algorithms for EEG-based brain-computer interfaces. *J Neural Eng* 2007; **4**:R1–R13.
8 Georgopoulos AP, Langheim FJ, Leuthold AC, Merkle AN. Magnetoencephalographic signals predict movement trajectory in space. *Exp Brain Res* 2005; **167**:132–135.
9 Das K, Giesbrecht B, Eckstein MP. Predicting variations of perceptual performance across individuals from neural activity using pattern classifiers. *Neuroimage* 2010; **51**:1425–1437.
10 Cheyne D, Weinberg H. Neuromagnetic fields accompanying unilateral finger movements: pre-movement and movement-evoked fields. *Exp Brain Res* 1989; **78**:604–612.
11 Kristeva R, Cheyne D, Deecke L. Neuromagnetic fields accompanying unilateral and bilateral voluntary movements: topography and analysis of cortical sources. *Electroencephalogr Clin Neurophysiol* 1991; **81**:284–298.
12 Cheyne D, Endo H, Takeda T, Weinberg H. Sensory feedback contributes to early movement-evoked fields during voluntary finger movements in humans. *Brain Res* 1997; **771**:196–202.
13 Cheyne D, Bakhtazad L, Gaetz W. Spatiotemporal mapping of cortical activity accompanying voluntary movements using an event-related beamforming approach. *Hum Brain Mapp* 2006; **27**:213–229.
14 Kristeva-Feige R, Rossi S, Pizzella V, Tecchio F, Romani GL, Erne S, *et al.* Neuromagnetic fields of the brain evoked by voluntary movement and electrical stimulation of the index finger. *Brain Res* 1995; **682**:22–28.
15 Erdler M, Beisteiner R, Mayer D, Kaindl T, Edward V, Windischberger C, *et al.* Supplementary motor area activation preceding voluntary movement is detectable with a whole-scalp magnetoencephalography system. *Neuroimage* 2000; **11**:697–707.
16 Kristeva-Feige R, Walter H, Lutkenhoner B, Hampson S, Ross B, Knorr U, *et al.* A neuromagnetic study of the functional organization of the sensorimotor cortex. *Eur J Neurosci* 1994; **6**:632–639.
17 Mayville JM, Fuchs A, Kelso JA. Neuromagnetic motor fields accompanying self-paced rhythmic finger movement at different rates. *Exp Brain Res* 2005; **166**:190–199.
18 Kamitani Y, Tong F. Decoding the visual and subjective contents of the human brain. *Nat Neurosci* 2005; **8**:679–685.
19 Kalaska JF, Scott SH, Cisek P, Sergio LE. Cortical control of reaching movements. *Curr Opin Neurobiol* 1997; **7**:849–859.
20 Haynes JD. Decoding and predicting intentions. *Ann N Y Acad Sci* 2011; **1224**:9–21.
21 Kakigi R, Hoshiyama M, Shimojo M, Naka D, Yamasaki H, Watanabe S, *et al.* The somatosensory evoked magnetic fields. *Prog Neurobiol* 2000; **61**: 495–523.
22 Hari R, Parkkonen L, Nangini C. The brain in time: insights from neuromagnetic recordings. *Ann N Y Acad Sci* 2010; **1191**:89–109.
23 Yanagisawa T, Hirata M, Saitoh Y, Kato A, Shibuya D, Kamitani Y, *et al.* Neural decoding using gyral and intrasulcal electrocorticograms. *Neuroimage* 2009; **45**:1099–1106.
24 Shoham S, Halgren E, Maynard EM, Normann RA. Motor-cortical activity in tetraplegics. *Nature* 2001; **413**:793.
25 Sabbah P, de SS, Leveque C, Gay S, Pfefer F, Nioche C, *et al.* Sensorimotor cortical activity in patients with complete spinal cord injury: a functional magnetic resonance imaging study. *J Neurotrauma* 2002; **19**:53–60.

Electrocorticographic Control of a Prosthetic Arm in Paralyzed Patients

Takufumi Yanagisawa, MD, PhD,[1,2] Masayuki Hirata, MD, PhD,[1] Youichi Saitoh, MD, PhD,[1,5] Haruhiko Kishima, MD, PhD,[1] Kojiro Matsushita, PhD,[1] Tetsu Goto, MD, PhD,[1] Ryohei Fukuma, MS,[2,3] Hiroshi Yokoi, PhD,[4] Yukiyasu Kamitani, PhD,[2,3] and Toshiki Yoshimine, MD, PhD[1]

Objective: Paralyzed patients may benefit from restoration of movement afforded by prosthetics controlled by electrocorticography (ECoG). Although ECoG shows promising results in human volunteers, it is unclear whether ECoG signals recorded from chronically paralyzed patients provide sufficient motor information, and if they do, whether they can be applied to control a prosthetic.

Methods: We recorded ECoG signals from sensorimotor cortices of 12 patients while they executed or attempted to execute 3 to 5 simple hand and elbow movements. Sensorimotor function was severely impaired in 3 patients due to peripheral nervous system lesion or amputation, moderately impaired due to central nervous system lesions sparing the cortex in 4 patients, and normal in 5 patients. Time frequency and decoding analyses were performed with the patients' ECoG signals.

Results: In all patients, the high gamma power (80–150Hz) of the ECoG signals during movements was clearly responsive to movement types and provided the best information for classifying different movement types. The classification performance was significantly better than chance in all patients, although differences between ECoG power modulations during different movement types were significantly less in patients with severely impaired motor function. In the impaired patients, cortical representations tended to overlap each other. Finally, using the classification method in real time, a moderately impaired patient and 3 nonparalyzed patients successfully controlled a prosthetic arm.

Interpretation: ECoG signals appear useful for prosthetic arm control and may provide clinically feasible motor restoration for patients with paralysis but no injury of the sensorimotor cortex.

ANN NEUROL 2012;71:353–361

Paralyzed patients and amputees would benefit from cortically controlled prosthetics in the form of a brain–computer interface (BCI). Among the possible cortical signals available for BCI, electrocorticography (ECoG) offers one of the most clinically feasible options, having superior long-term stability and lower technical difficulty compared with other invasive signals.[1,2] Evidence from studies with nonparetic patients with epilepsy shows that some movements or movement intentions can be inferred from ECoG signals accurately enough to control external devices such as a computer cursor.[3–6] However, it is unclear whether these findings are applicable to paralyzed patients, whose sensorimotor cortices may have undergone extensive reorganization after deefferentation and deafferentation of the paralyzed body parts.

Paresis-associated cortical reorganization may modify ECoG signals of the sensorimotor cortex. Cortical reorganization occurs in the sensorimotor cortex of individuals with spinal cord injuries,[7–9] limb amputations,[10–12] and stroke.[13–15] Such cortical reorganizations have been shown to alter functional activations in the

View this article online at wileyonlinelibrary.com. DOI: 10.1002/ana.22613

Received Feb 4, 2011, and in revised form Aug 4, 2011. Accepted for publication Aug 12, 2011.

Address correspondence to Dr Hirata, Department of Neurosurgery, Osaka University Medical School, E6 2-2 Yamadaoka Suita, Osaka, Japan. E-mail: mhirata@nsurg.med.osaka-u.ac.jp or Dr Kamitani, ATR Computational Neuroscience Laboratories, 2-2-2 Hikaridai, Seika, Soraku, Kyoto 619-0288, Japan. E-mail: kmtn@atr.jp

[1]Department of Neurosurgery, Osaka University Medical School, Osaka; [2]ATR Computational Neuroscience Laboratories, Kyoto; [3]Nara Institute of Science and Technology, Nara; and [4]University of Tokyo Interfaculty Initiative in Information Studies Graduate School of Interdisciplinary Information Studies, Tokyo, Japan; [5]Department of Neuromodulation and Neurosurgery office for University-Industry Collaboration, Osaka, Japan.

Additional supporting information can be found in the online version of this article.

TABLE 1: Clinical Profiles

Patient No.	Age, yr/Sex	Diagnosis	Duration of Disease, yr	Paresis in Affected Limb (MMT)	Sensation in Affected Limb
N1	34/F	R intractable epilepsy	19	None	Normal
N2	14/M	R intractable epilepsy	7	None	Normal
N3	20/F	L intractable epilepsy	6	None	Normal
N4	22/F	R intractable epilepsy	10	None	Normal
N5	13/M	L intractable epilepsy	11	None	Normal
P1	49/M	R putaminal hemorrhage	2	Slightly spastic (5−)	Hypoesthesia
P2	66/F	R subcortical infarction	3.3	Spastic (4)	Hypoesthesia
P3	64/M	R thalamic hemorrhage	7	Spastic (4)	Hypoesthesia
P4	65/M	Ruptured spinal dAVF	8	Spastic (4)	Hypoesthesia
S1	31/M	L brachial plexus avulsion	5	Complete (0)[a]	Anesthesia
S2	49/M	L brachial plexus avulsion	6	Severe (1)[a]	Severe hypoesthesia
S3	47/M	Amputation below L shoulder	3.3	No arm	None

[a]Post transplantation of intercostal nerve.
dAVF = dural arteriovenous fistula; F = female; L = left; M = male; MMT = manual muscle test; R = right.

cortices and affect motor function,[14] sensation, and recognition of body parts.[10,11,16] However, quantitative data are lacking on altered functional activations of the sensorimotor cortex after cortical reorganization and subsequent modification of ECoG signals.

We examined ECoG signals of nonparalyzed patients and patients with different levels of motor dysfunctions to quantitatively address 3 questions: (1) Do the ECoG signals of patients with chronic motor dysfunctions show preservation of spatiotemporal patterns of activation even after reorganization? (2) How much are ECoG activation maps for different motor tasks modified in the reorganized sensorimotor cortex? and (3) Can ECoG activation be applicable to controlling a prosthetic arm?

Patients and Methods

Patient Population

Twelve patients (4 female, 8 male; age range, 13–66 years) with subdural electrodes participated in this study. The patients had different degrees of motor dysfunctions and sensory disturbances (Table 1). Five patients (N1–N5) with epilepsy had no motor dysfunctions; 4 patients (P1–P4) had spastic paresis and weakness in their upper limbs due to strokes without damage to the sensorimotor cortex (moderate motor dysfunction); and 3 patients (S1–S3) had severely impaired sensorimotor function of their limbs due to brachial plexus root avulsion or amputation (severe motor dysfunction; Supplementary Methods). Patients S1–S3 differed in their ability to imagine movement of their affected limbs (Table 2). All participants or their guardians gave written informed consent to participate in the study, which was approved by the ethics committee of Osaka University Hospital.

All patients had been implanted with subdural electrode arrays that covered a broad sensorimotor cortical area, including the hand motor strip. These arrays were kept in place for 2 weeks to determine either the epileptic foci or the optimal stimulation sites to achieve maximum pain reduction.[17] At the end of these 2 weeks, the arrays were removed. In impaired patients, 4 permanent electrodes were then placed at the sites where stimulation provided optimal pain control.

Movement Tasks

Experiments were performed in an electromagnetically shielded room approximately 1 week after electrode placement. The first session was designed to train the decoder on the ECoG signals (decoder training session). Patients performed 1 of 3 possible movement tasks that differed by the set of movement types that were executed: (1) grasping, thumb flexion, and elbow flexion (P1, P2, S1–S3); (2) grasping, pinching, hand-opening, elbow flexion, and tongue protrusion (P3); or (3) grasping, pinching, hand-opening, elbow flexion, and elbow extension (N1–N5, P4). For movement task 3, the patients were first instructed to perform the 3 hand movements. Then, after a free-run session in which patients undertook movements at their own pace, if they were able to undertake additional sessions without fatigue, they were instructed to perform 5 movements, preferably ones involving the elbow. Grasping and elbow flexion were commonly performed among all patients, although we selected the

TABLE 2: Summary of the Decoding Results

Patient No.	Ability to Imagine Movements	% Correct (grasp vs elbow)	Mean ± SD	% Correct (move vs rest)	Mean ± SD
N1		92.9	92.5 ± 3.4 ($p < 0.05$)	96.6	93.6 ± 4.4 (NS)
N2		98.2		94.5	
N3		90.7		86.0	
N4		90.5		94.2	
N5		90.0		96.4	
P1		86.7	89.2 ± 5.8 (NS)	95.7	95.6 ± 4.5 (NS)
P2		85.7		100.0	
P3		97.9		89.5	
P4		86.7		97.3	
S1	Easy	90.3	71.3 ± 17.0 ($p < 0.05$)	98.2	93.2 ± 4.6 (NS)
S2	Slightly difficult	57.3		92.2	
S3	Difficult	66.3		89.2	

NS = not significant; SD = standard deviation.

3 types of movement tasks to adjust the way patients could control the prosthesis.

The patients selected and performed one of the movements within a presented task after being cued with auditory beeps (Fig 1A). The patients were instructed to execute movements immediately after the third beep and then return their hands or elbows to a resting position. For the resting position, patients were instructed to relax their hands or elbows with slightly flexed joints. Each type of movement was performed approximately 30 to 100 times. Patients S1–S3 were instructed to attempt the movements of their affected limbs immediately after the auditory cue. The movement instructions were delivered using a PC monitor controlled by ViSaGe (Cambridge Research System, Rochester, UK) placed in front of the patients. The decoder training session was open loop. The patients were not informed of the classifier results and therefore did not have an opportunity for learning or improving their performance.

After the decoder training session, 4 patients repeated the same task they had performed during the session, but at self-paced intervals without external cues (free-run session, see Fig 1B). These patients had recently performed the task and were able to continue without extensive fatigue. Without receiving further training, they were instructed to control the prosthetic arm by performing their hand and elbow movements. Patient N1 could not control the elbow of the prosthetic arm due to mechanical problems of the prosthesis.

ECoG Recording and Preprocessing

For each patient, 15 to 60 planar-surface platinum grid electrodes were placed over the sensorimotor cortex and within the central sulcus (intrasulcal electrodes)[18] (see Supplementary Methods). Video recording and electromyographic (EMG electrode; Nihon Koden, Tokyo, Japan) recordings of their hands and arms were performed solely to identify the performed movements.

ECoGs were recorded and digitized at a sampling rate of 1,000Hz. During the decoder training session, the ECoG signals were obtained time-locked to the cue signal. In the free-run session, 1-second duration ECoG signals were recorded online at 200-millisecond intervals. A fast Fourier transformation (FFT; EEGLAB v5.03) was performed for each 1-second signal to obtain the power of each of the 3 frequency bands (2–8, 8–25, and 80–150Hz) for each electrode. We used FFT to complete the online decoding over the 200 milliseconds. The 3 frequency bands were chosen based on our previous studies.[19]

Decoding Algorithms and Prosthetic Hand Control

To infer, or decode, the movement types executed or attempted by the patients, we constructed a linear classifier trained by a linear support vector machine, the SVM decoder (see Supplementary Methods).[18,20,21] The trained SVM decoder was inputted with the ECoG signals to output an inferred movement type. A 5-fold cross-validation was used to test how well the decoder could generalize.

To apply the SVM decoder to the free-run sessions without external cues, we developed another decoder (GPR decoder; see Supplementary Methods). The trained GPR decoder was also inputted with the ECoG signals to output an estimated

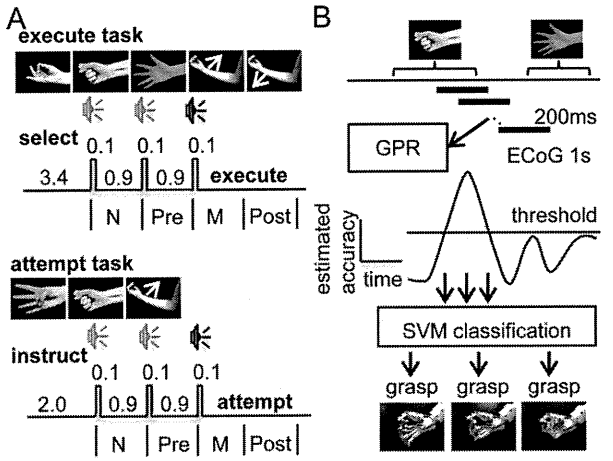

FIGURE 1: Task paradigm. (A) The task paradigm during the decoder training session. In the execute task, patients selected and executed 1 of 3 (or 5) movements after the sound cue. The cue consisted of 3 beeps 1 second apart that recurred every 5.5 seconds. The movements were performed with the arm contralateral to the implanted electrodes. In the attempt task, patients were instructed which of the 3 (or 5) movements to attempt. The 1-second electrocorticography (ECoG) signals used for the decoding analysis are shown below the time line: N = used for normalization and resting state; Pre = used as the first period by the Gaussian process regression (GPR) decoder; M = used as the move state; Post = as the last period by the GPR decoder. (B) Controlling the prosthetic hand with 2 decoders. The GPR decoder estimated the accuracy of the time determined to be necessary for the support vector machine (SVM) decoder to classify the ECoG signals. The prosthetic hand was controlled incrementally according to the decoding results.

classification accuracy of the SVM decoder. When the estimated classification accuracy exceeded a certain threshold value (see Fig 1B), the SVM decoder classified the ECoG signals to infer the intended movement (Supplementary Fig 3).

The GPR decoder was trained using a Gaussian process regression (GPR),[22] which is one kind of Bayesian approach.[23] We used GPR because it could be applied to the nonlinear data with a simple model. The GPR decoder was trained with the classification accuracies and the 3 frequency band powers of 3 time domains (Pre, M, and Post in Fig 1A; see Supplementary Methods). The classification accuracies were evaluated by the mutual information, which quantified the confusion matrix resulting from the SVM decoder. The mutual information was normalized by using the values of the 3 time domains. The trained GPR decoder estimated the classification accuracy with 3 frequency band powers at a given time in a free-run session. The GPR and SVM decoders were trained for hand and elbow movements separately.

The commands to the prosthetic arm were updated by the host computer system every 200 milliseconds. When the SVM decoder inferred a movement type, the posture of the prosthetic arm was partially altered to match the posture of the inferred movement (see Supplementary Methods). Completing a movement required 2 or 3 consecutive matched decodings. This incremental control of the prosthetic hand permitted the desired posture even when the classification performance of the SVM decoder was not perfect; the classification errors of the

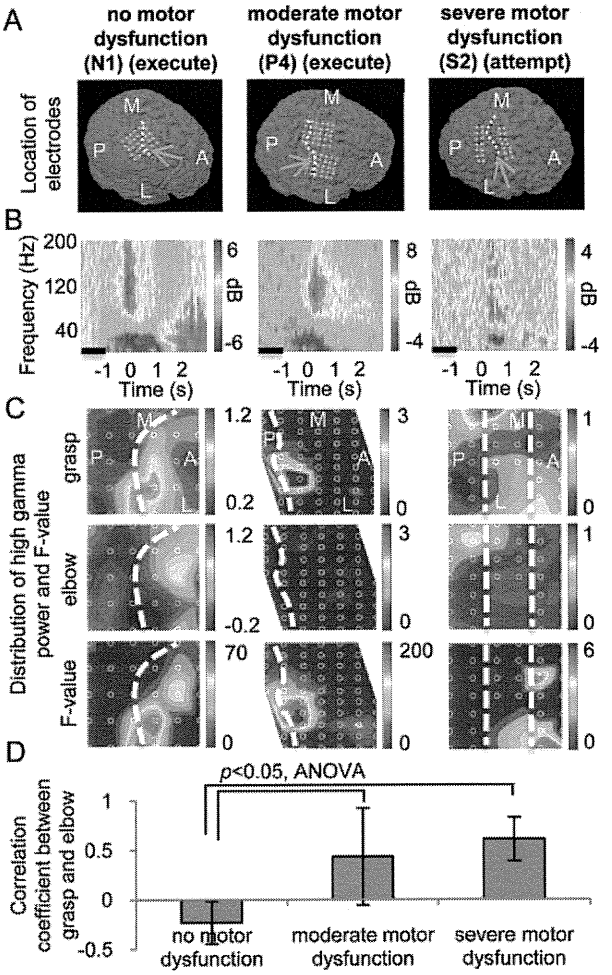

FIGURE 2: Representative results of time-frequency analysis. (A) Locations of implanted electrodes for patients N1, P4, and S2 are indicated by the green (implanted on the brain surface) and red (implanted within the central sulcus) filled circles on the 3-dimensional brain renderings of magnetic resonance imaging volumes. The dashed white line indicates the location of the central sulcus. Only the electrodes used for the analysis are shown. (B) Power spectra of the electrocorticographic signals recorded during grasping (execute) or attempt to grasp from the electrodes on the primary motor cortex indicated by the orange arrows in A. The black horizontal bars show the 1,000-millisecond period used for normalization. Time 0 corresponds to the onset cue. (C) The high gamma power is color coded to the location of the electrodes for grasping and elbow flexion. The direction indicators correspond to A = anterior, P = posterior, M = medial, and L = lateral on the brain. The white dashed lines and the white circles indicate the locations of the central sulcus and the electrodes, respectively. For the patient S2, the electrodes between the 2 white lines were located within the central sulcus (intrasulcal electrodes; see Supplementary Methods). The lowest figure of each patient shows the distribution of the *F* value with statistical significance ($p < 0.05$). (D) The correlation coefficient of the high gamma powers between hand grasping and elbow flexion for each patient's group. ANOVA = analysis of variance.

decoder caused only a tremor of the prosthetic arm as it moved to the desired posture.

Offline Analyses

The ECoG signals of grasping and elbow flexion were compared among patients. A Hilbert transformation (EEGLAB v5.03) was used to obtain the temporal power spectral density of each frequency band (see Supplementary Methods). The temporal powers were normalized by powers of the initial 1-second period (−2 to −1 seconds) of each trial.

The variability of the high gamma power of 0 to 1 second was statistically evaluated among 2 types of movements by the F value of one-way analysis of variance (ANOVA) for each electrode. The statistical similarity of the high gamma power maps was evaluated by determining the correlation coefficient of the mean power maps of 2 movements. The classification accuracies for inferring 2 movements using the SVM decoder with the high gamma powers were compared among patients.

Results

Time-Frequency Analysis

The power spectrum of the ECoG signals showed some characteristic modulations among patients. Figure 2B illustrates examples of the power spectrum time-locked to the external cues while grasping or attempting to grasp. An increase in the high gamma power and decreases in the alpha and beta powers were consistently observed for all patients with different levels of motor dysfunctions. The spatial distributions of the high gamma power during movement (0–1 second) were obviously different for each movement (see Fig 2C), and the ANOVA F value revealed that high gamma powers were significantly modulated between the movements. Notably, the powers around the central sulcus showed significant differences ($p < 0.05$). The characteristic modulations of the high gamma power were consistently observed among all patients, although the F values pertaining to variability were lower in patients with severe dysfunctions than in other patients. Moreover, the correlation coefficient of the spatial distribution of the high gamma power between the movements was significantly high for the patients with motor dysfunctions (see Fig 2D).

Decoding Analysis

The accuracy of classifying (ie, decoding) the movements was compared among the frequency band powers at each time. Figure 3 shows the color-coded percentage of correct movement classifications averaged over each patient group. Regardless of the level of motor dysfunctions, the 2 movement types were best inferred by using the high gamma power around the movement onset.

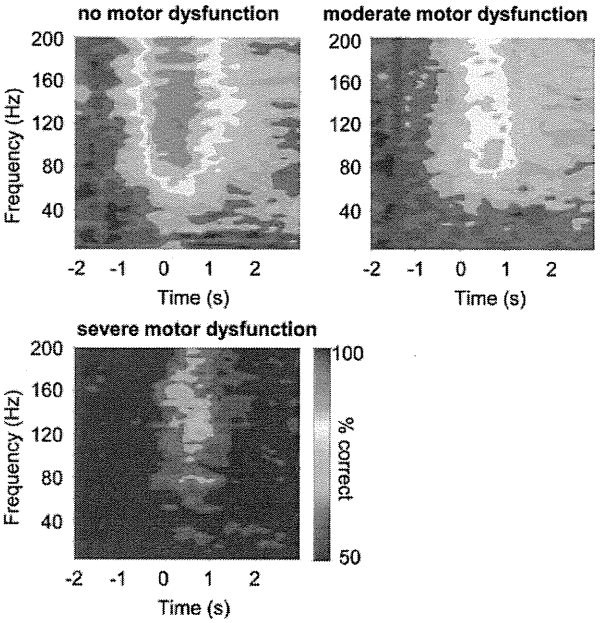

FIGURE 3: Averaged classification accuracy with each frequency band power. Classification accuracies with each frequency band power were averaged for the patients of each group and color coded at the center of each frequency band and time domain. Time 0 corresponds to the sound cue for the movements.

The movement classifications were carried out for all patients with a high gamma power for 0 to 1 seconds. The classification accuracy of patients S1 to S3 was significantly inferior to that of patients N1 to N5 (ANOVA, $p < 0.05$; see Table 2). However, these accuracies were still above levels that would occur by chance (50%). This relationship was also observed in the classification of 3 types of movements (Supplementary Table). On the other hand, the accuracies to classify the resting state (−2 to −1 seconds) and the movement state (0 to 1 seconds) were not significantly different among the 3 patient groups (see Table 2).

Decoding in Free-Run and Real-Time Control of a Prosthetic Hand

The classification accuracy of 3 hand movements with the SVM decoder varied with time in the decoder training session (Fig 4B). It was highest immediately after the onset cues (eg, when the hand EMG response started to increase; see Fig 4A). The trained GPR decoder accurately inferred the timing of the peak and zero value of the normalized mutual information only using the 3 frequency bands at each time (see Fig 4C).

Using the trained decoders, the ECoG signals were decoded in real time while the patient, without further training, voluntarily (ie, without cue) performed the 3 to 5 types of movements (free-run period, see Fig 4D). The estimated mutual information peaked when the standard

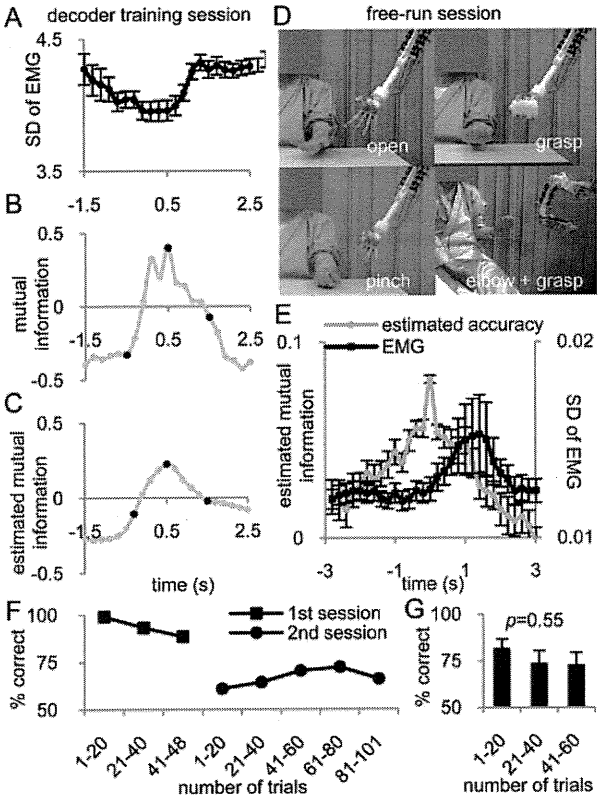

FIGURE 4: Prosthetic control with the electrocorticography (ECoG) signals. (A) The standard deviations (SDs) of the electromyographic (EMG) responses averaged over 1-second periods are shown at each time centered on the onset cue (0). (B) For patient P4, the mutual information for the performed movements and the inferred movements was normalized at each time. The values of the mutual information at 3 time domains (black circle) trained the Gaussian process regression (GPR) decoder. (C) The mutual information estimated by the trained GPR decoder at each time. (D) Representative photographs of the prosthetic arm controlled in real time by the ECoG signals of patient P4. (E) The estimated mutual information and standard deviation of the EMG responses were averaged for the 6 seconds time-locked to the peak values of the estimated mutual information that exceeded a value of 0.07. (F) The percentage correct of each 20 trials over the course of the entire free-run session of P4 (squares = first session; circles = second session). (G) The percentage correct of each 20 trials were not significantly different among all sessions of 4 patients (analysis of variance, $p = 0.55$).

deviation of the EMG response started to increase, indicating that the GPR decoder successfully decoded the movement onset in the free-run session (see Fig 4E).

The prosthetic arm was controlled in real time according to the decoding results of the SVM and GPR decoders, mimicking the hand movements of patients. The prosthetic hand completed the same movement of patient P4 in 42 of 48 attempts (87.5%; Supplementary Video 1). Each hand movement required an average of 2.2 incremental movements of 4.2 seconds each. By voluntarily moving his own hand, patient P4 was able to catch and hold an object for seconds and intentionally release the object from the prosthetic hand (Supplementary Video 2). Moreover 4 days after the first experiments (second free run), the patient was still able to perform the same free-run task (Table 3, see Fig 4F, Supplementary Video 3), using the decoder trained in those initial experiments. The 3 other participating patients (N1, N3, N4) were also able to voluntarily control the prosthetic arm (see Table 3). Notably, the classification accuracy of the SVM decoder was not significantly different between the training session and the free-run session (ANOVA, $p = 0.06$) and over the course of the each free-run session (ANOVA, $p = 0.55$; see Fig 4F, G). Finally, the elbow of the prosthetic arm was simultaneously controlled by the other GPR decoder for the elbow (Supplementary Video 4). The success rate for complete elbow movements of the prosthetic arm was significantly lower than that of the training (ANOVA, $p < 0.05$).

Patient N1 described her impression of control as thinking at first that the prosthetic arm moved in mimicry of her movements, rather than that she was controlling the prosthesis. But at the end of the experiment, she realized she was able to control the prosthesis well. However, no patient controlling the prosthesis stopped moving their own limb.

Discussion

We have shown that ECoG signals recorded from patients with chronic motor dysfunctions still represented motor information via high gamma power to a degree that they could be decoded successfully enough to control a prosthetic hand. However, the modulation of the representation for different movements may have deteriorated depending on the degree of impairment. Our quantitative evaluation of motor representations in the reorganized cortex elucidated pathological states of patients with motor dysfunctions and demonstrated the applicability of these representations for an ECoG-based BCI to improve patients' quality of life.

Preserved Features following Cortical Reorganization

The spatiotemporal features of the ECoG signals during movements or attempts at movements were qualitatively preserved in the sensorimotor cortex of impaired patients. During movements, high gamma power was consistently increased around the central sulcus, even for severely impaired patients. This is consistent with previous functional magnetic resonance imaging (fMRI) studies showing that activation of the motor cortex is

TABLE 3: Summary of the Real-Time Control of the Prosthetic Hand

Patient No. and Session		Hand Movements (grasp, pinch, open)				Elbow Movements (flexion, extension)			
		% Correct of Training	% Correct to Complete (correct/trial)	% Correct of SVM Decoder in Free Run	Time/Count to Complete (s/count)	% Correct of Training	% Correct to Complete (correct/trial)	% Correct of SVM Decoder in Free Run	Time/Count to Complete (s/count)
N1	1st	79.2	71.2 (37/52)	76.1	1.8/3.3	64.3	—	—	—
	2nd		51.2 (22/43)	67.0	1.5/3.3				
N3	1st	70.0	85.7 (30/35)	80.7	1.6/3.3	77.5	14.3 (1/7)	87.5	13.6/3
	2nd		47.2 (17/36)	81.0	1.3/2.7				
N4	1st	60.8	64.7 (11/17)	70.3	1.3/3.7	74.0	33.3 (1/3)	60.0	3.3/2
	2nd		—	—	—				
P4	1st	80.8	87.5 (42/48)	68.8	2.2/4.2	70.0	54.2 (26/48)	90.1	2.3/3.7
	2nd		62.3 (63/101)	62.3	2.0/4.1				
Mean ± SD		72.7 ± 9.2	77.3 ± 11.1	74.0 ± 5.5	1.7 ± 0.4/ 3.6 ± 0.4	71.5 ± 5.7	33.9 ± 20.0 ($p < 0.05$, ANOVA)	79.2 ± 16.7	6.4 ± .6.3/ 2.9 ± 0.9
			53.6 ± 7.8	70.1 ± 9.7	1.6 ± 0.4/ 3.6 ± 0.7				

ANOVA = analysis of variance; SVM = support vector machine.

preserved even in paralyzed patients,[24–26] because the high gamma activity is correlated with the fMRI blood oxygen level-dependent signal.[27]

The decoding analysis showed that modulation of the high gamma power provided the most information about the movement types. This result was consistent with previous studies that showed human movements could be inferred by using ECoGs.[3,4,28,29] It was suggested that the basic features of cortical processing with high gamma powers are preserved following cortical reorganization resulting from motor dysfunctions.

Deteriorated Motor Representation Accompanying Phantom Limb Pain

The decreased decoding accuracy in patients with motor dysfunctions indicated that the high gamma powers were not prominently modulated among the different types of movements, suggesting that modulation of the high gamma power (ie, motor representation) had significantly deteriorated following cortical reorganization. Conversely, the increased correlation of the high gamma powers between different movements suggested that the representations of the movements became similar to each other in the impaired patients. Notably, this similarity was not due to a weakened representation; an increase in the high gamma power during movement was accurately decoded even in the patients with severe dysfunctions. Our results suggested that the modulation of the high gamma powers had deteriorated in the impaired patients with increased similarity of the power maps among movements. This result was consistent with previous reports showing that cortical representations of nonaffected body parts shifted to overlap representations of affected body parts in phantom limb pain patients.[11,16,30] It was suggested that the decreased decoding accuracy of movement types might be due to overlaps in the spatial distributions of the high gamma powers for each movement.

Our data also suggested that the deteriorated modulation of motor representations in patients S1 to S3 was related to patients' ability to imagine movements. Classification accuracy of these patients was highest for the patient who could most easily imagine the movements and lowest for the patients who could hardly imagine movements. This relation was also observed in the distribution of the F values of the high gamma powers (Supplementary Fig 4). For some patients who lost the ability to imagine intentionally moving their phantom limbs, the motor representation, or high gamma powers, may no longer be modulated well enough to be decoded. We suggest that cortical reorganization did not alter the characteristic features of the ECoG signals, but rather affected modulation of the representation, related to the ability to imagine the movements.

Prosthetic Hand Control Applied to a Diverse Patient Population

Successful control of the prosthetic arm was demonstrated with the SVM and GPR decoders, which accurately inferred various movement types from the ECoG signals of patients with motor dysfunctions. This suggests the feasibility of restoring purposeful movement based on a BCI. Although the cortical control of some prostheses has already been demonstrated with other invasive signals,[31,32] our success with the ECoG signals may be beneficial for clinical applications because an ECoG-based BCI has advantages in signal stability and durability that are absolutely necessary for clinical application.[2] As we demonstrated, the prosthetic hand could be controlled for several days with a single decoder trained once at the first session. This reveals the robustness of our decoding method and the stability of the ECoG signals. Moreover, our method was demonstrated with an elderly patient who was able to successfully and naturally control the prosthetic arm without any prior training. A requisite for a clinically useful BCI system is that it be developed to be stably and easily used by a diverse population of patients in their daily lives.

Acknowledgments

This work was supported in part by the Strategic Research Program for Brain Sciences of Ministry of Education, Culture, Sports, Science and Technology-Japan (MEXT); KAKENHI (22700435); Nissan Science Foundation; Ministry of Health, Labor, and Welfare (18261201); and Strategic Information and Communications R&D promotion Programme (SCOPE), SOUMU.

Potential Conflicts of Interest

Nothing to report.

References

1. Leuthardt EC, Schalk G, Moran D, et al. The emerging world of motor neuroprosthetics: a neurosurgical perspective. Neurosurgery 2006;59:1–14.
2. Chao ZC, Nagasaka Y, Fujii N. Long-term asynchronous decoding of arm motion using electrocorticographic signals in monkeys. Front Neuroeng 2010;3:3.
3. Pistohl T, Ball T, Schulze-Bonhage A, et al. Prediction of arm movement trajectories from ECoG-recordings in humans. J Neurosci Methods 2008;167:105–114.
4. Schalk G, Miller KJ, Anderson NR, et al. Two-dimensional movement control using electrocorticographic signals in humans. J Neural Eng 2008;5:75–84.
5. Schalk G, Kubanek J, Miller KJ, et al. Two-dimensional movement trajectories using electrocorticographic signals in humans. J Neural Eng 2007;4:264–275.

6. Miller KJ, Zanos S, Fetz EE, et al. Decoupling the cortical power spectrum reveals real-time representation of individual finger movements in humans. J Neurosci 2009;29:3132–3137.
7. Bruehlmeier M, Dietz V, Leenders KL, et al. How does the human brain deal with a spinal cord injury? Eur J Neurosci 1998;10: 3918–3922.
8. Green JB, Sora E, Bialy Y, et al. Cortical motor reorganization after paraplegia: an EEG study. Neurology 1999;53:736–743.
9. Mikulis DJ, Jurkiewicz MT, McIlroy WE, et al. Adaptation in the motor cortex following cervical spinal cord injury. Neurology 2002;58:794–801.
10. Ramachandran VS, Rogers-Ramachandran D, Stewart M. Perceptual correlates of massive cortical reorganization. Science 1992; 258:1159–1160.
11. Flor H. Phantom-limb pain: characteristics, causes, and treatment. Lancet Neurol 2002;1:182–189.
12. Roricht S, Meyer BU, Niehaus L, et al. Long-term reorganization of motor cortex outputs after arm amputation. Neurology 1999;53:106–111.
13. Green JB. Brain reorganization after stroke. Top Stroke Rehabil 2003;10:1–20.
14. Nudo RJ, Wise BM, SiFuentes F, et al. Neural substrates for the effects of rehabilitative training on motor recovery after ischemic infarct. Science 1996;272:1791–1794.
15. Gerloff C, Bushara K, Sailer A, et al. Multimodal imaging of brain reorganization in motor areas of the contralesional hemisphere of well recovered patients after capsular stroke. Brain 2006;129:791–808.
16. Flor H, Elbert T, Knecht S, et al. Phantom-limb pain as a perceptual correlate of cortical reorganization following arm amputation. Nature 1995;375:482–484.
17. Hosomi K, Saitoh Y, Kishima H, et al. Electrical stimulation of primary motor cortex within the central sulcus for intractable neuropathic pain. Clin Neurophysiol 2008;119:993–1001.
18. Yanagisawa T, Hirata M, Saitoh Y, et al. Neural decoding using gyral and intrasulcal electrocorticograms. Neuroimage 2009;45:1099–1106.
19. Yanagisawa T, Hirata M, Saitoh Y, et al. Real-time control of a prosthetic hand using human electrocorticography signals. J Neurosurg 2011;114:1715–1722.
20. Kamitani Y, Tong F. Decoding the visual and subjective contents of the human brain. Nat Neurosci 2005;8:679–685.
21. Kamitani Y. Brain decoder toolbox. 2010. Available at: http://www.cns.atr.jp/dni/en/downloads/brain-decoder-toolbox. Assessed on 12 May 2010.
22. Ebden M. Gaussian processes for regression: a quick introduction. Available at: http://www.robots.ox.ac.uk/~mebden/reports/GPtutorial.pdf. Assessed on 15 December 2010
23. Rasmussen C, Williams C. Gaussian processes for machine learning. Cambridge, MA: MIT Press, 2006.
24. Shoham S, Halgren E, Maynard EM, et al. Motor-cortical activity in tetraplegics. Nature 2001;413:793.
25. Corbetta M, Burton H, Sinclair RJ, et al. Functional reorganization and stability of somatosensory-motor cortical topography in a tetraplegic subject with late recovery. Proc Natl Acad Sci USA 2002; 99:17066–17071.
26. Cramer SC, Lastra L, Lacourse MG, et al. Brain motor system function after chronic, complete spinal cord injury. Brain 2005;128: 2941–2950.
27. Logothetis NK, Pauls J, Augath M, et al. Neurophysiological investigation of the basis of the fMRI signal. Nature 2001;412: 150–157.
28. Kubanek J, Miller KJ, Ojemann JG, et al. Decoding flexion of individual fingers using electrocorticographic signals in humans. J Neural Eng 2009;6:1–14.
29. Crone NE, Sinai A, Korzeniewska A. High-frequency gamma oscillations and human brain mapping with electrocorticography. Prog Brain Res 2006;159:275–295.
30. Karl A, Birbaumer N, Lutzengerger W, et al. Reorganization of motor and somatosensory cortex in upper extremity amputees with phantom limb pain. J Neurosci 2001;21:3609–3618.
31. Velliste M, Perel S, Spalding MC, et al. Cortical control of a prosthetic arm for self-feeding. Nature 2008;453:1098–1101.
32. Hochberg LR, Serruya MD, Friehs GM, et al. Neuronal ensemble control of prosthetic devices by a human with tetraplegia. Nature 2006;442:164–171.

///VSP///

Advanced Robotics 26 (2012) 399–408

ADVANCED ROBOTICS
brill.nl/ar

Short paper

Motor Restoration Based on the Brain–Machine Interface Using Brain Surface Electrodes: Real-Time Robot Control and a Fully Implantable Wireless System

Masayuki Hirata [a,*], Kojiro Matsushita [a], Takufumi Yanagisawa [a], Tetsu Goto [a], Shayne Morris [a], Hiroshi Yokoi [b], Takafumi Suzuki [c], Takeshi Yoshida [d], Fumihiro Sato [e], Osamu Sakura [b], Yukiyasu Kamitani [f] and Toshiki Yoshimine [a]

[a] Department of Neurosurgery, Osaka University Medical School, Suita-shi, Osaka 565-0871, Japan
[b] University of Tokyo Interfaculty Initiative in Information Studies, Graduate School of Interdisciplinary Information Studies, Hongo 7-3-1, Bunkyo-ku, Tokyo 113-0033, Japan
[c] Graduate School of Information Science and Technology, University of Tokyo, Bunkyo-ku, Tokyo 113-0033, Japan
[d] Graduate School of Advanced Sciences of Matter, Hiroshima University, Higashihiroshima, Hiroshima 739-8530, Japan
[e] Group of Electrical Engineering, Communication Engineering, Electronic Engineering and Information Engineering, Tohoku University, Sendai, Miyagi 980-8578, Japan
[f] ATR Computational Neuroscience Laboratories, Soraku-gun, Kyoto 619-0288, Japan

Received 12 April 2011; accepted 7 June 2011

Abstract

The brain–machine interface (BMI) is a new approach to the man–machine interface, which enables us to control machines and to communicate with others without input devices, but directly using brain signals. We describe our integrative approach to develop a BMI system using brain surface electrodes for motor and communication control in severely disabled people. This includes effective brain signal recording, accurate neural decoding, robust robot control, a wireless fully implantable device, a non-invasive evaluation of surgical indications, etc. In addition, the inspection and addressing of neuroethical issues is indispensible when undertaking work in this field.

Keywords

Brain–machine interface, neural decoding, real-time, prosthetic arm, implantable device

* To whom correspondence should be addressed. E-mail: mhirata@nsurg.med.osaka-u.ac.jp

DOI:10.1163/156855311X614581

1. Introduction

The brain–machine interface (BMI) is a new approach to the man–machine interface, which enables us to control machines and communicate with others without input devices, but directly using brain signals alone (Fig. 1). There are many diseases and conditions that lead to a loss of muscular control without disruption of the patients' cognitive abilities. These include amyotrophic lateral sclerosis, brainstem stroke, spinal cord injury, muscular dystrophy, Parkinson's disease, cerebral palsy, etc. BMI technology can offer these patients greater independence and a higher quality of life by enabling the control of external devices to communicate with others and to manipulate their environment according to their will [1]. Functional restoration using the BMI is a more feasible solution in the shorter term when compared to methods using neural regeneration or neural transplantation, which presently lack the critical technologies necessary to organize functional neural networks.

There are two types of BMI — invasive and non-invasive. The invasive BMI requires surgical procedures and measures brain signals from intracranial electrodes (needle electrodes or brain surface electrodes), while the non-invasive BMI measures brain signals non-invasively from outside of the body using scalp electrodes, etc. To achieve higher performance, and, thus, usefulness, we use invasive BMI techniques that involve the implantation of devices. For use in a practical situation, the invasive BMI needs organic integration of the following medical and engineering technologies:

(i) Neural recording with high spatiotemporal resolution.

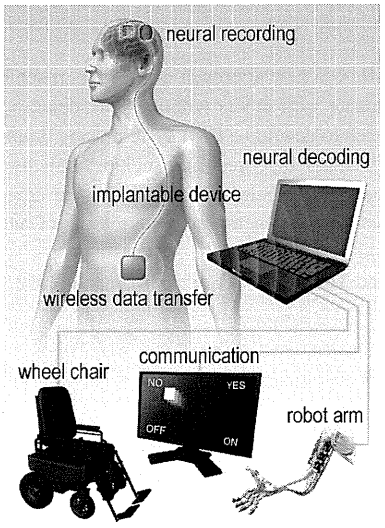

Figure 1. Conceptual diagram of the BMI.

(ii) High-speed transfer and processing of neural signals.

(iii) Optimal extraction of neurophysiological features.

(iv) Neural decoding.

(v) Control of external devices such as robots.

(vi) Downsizing, integration and implantation of electronic devices, and the use of wireless technology.

(vii) Non-invasive evaluations for appropriate surgical indications.

(viii) On-target survey and analysis of patient needs.

(ix) Addressing neuroethical issues.

In this paper, we describe the development of our invasive BMI system using brain surface electrodes.

2. Neural Decoding and Real-Time Robot Control Using Electrocorticograms

In the process of providing neurosurgical treatments for certain groups of patients, we sometimes record brain signals (electrocorticograms (ECoGs)) or electrically stimulate the brain using electrodes directly placed on the brain surface. ECoGs selectively measure brain signals within the limited distance of a few millimeters without distortion and are, in addition, not susceptible to external noises, while scalp skin electrodes measure distorted brain signals from a distance of up to a few centimeters. Thus, we prefer to use ECoGs recorded by brain surface electrodes for the BMI to achieve high performance.

Eighteen subjects have participated in the present studies to date. All of the subjects were recruited from patients in whom we temporarily had to place brain surface electrodes in order to treat intractable pain or intractable epilepsy. Informed consent was obtained from all of the patients. All studies were performed with the approval of the Ethics Committee of Osaka University Medical Hospital. We measured ECoGs during two or three types of simple motor tasks of the hand or the arm, such as grasping, pinching and elbow flexion. We predicted the type of movement based on analysis of single-trial ECoGs using a support vector machine (SVM) algorithm [2]. As a result, we were able to predict movement types on a single-trial basis with an accuracy rate of 70–90%. Specifically, we first demonstrated that ECoGs from the anterior wall of the central sulcus (the groove in the brain where most of the primary motor cortex lies) are useful for the accurate and early decoding of the movement types [3]. Most of the primary motor cortex, which is responsible for the final output portion of motor commands, lies within the anterior wall of the central sulcus. Especially in the human, the anterior wall of the central sulcus has many neurons directly projecting to the spinal anterior horn cells. Such neurons are thought to be related to fine movement control [4]. We suppose that appropri-

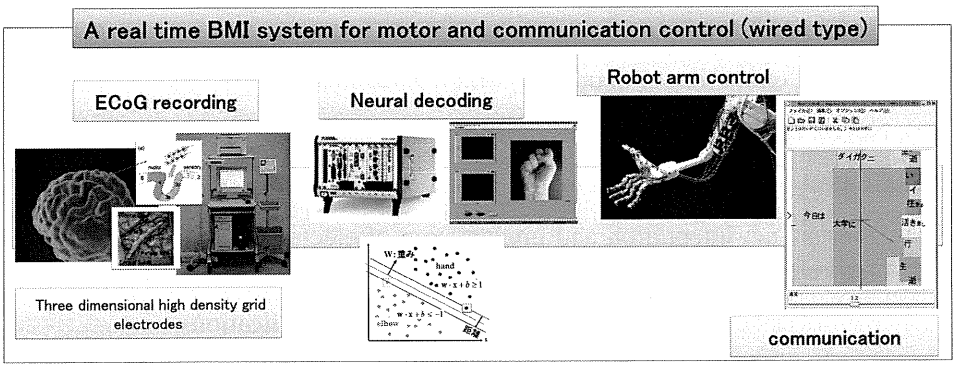

Figure 2. Real-time BMI system for motor and communication control (wired type).

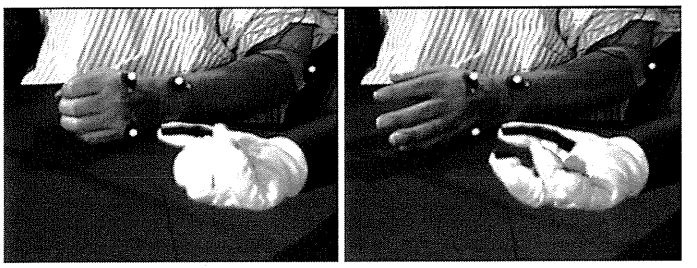

Figure 3. Real-time control of a robot hand. The patient voluntarily controlled grasping (left) and opening (right) the robot hand in real-time.

ate neurophysiological feature extraction from the central sulcus contributed to our accurate movement decoding.

We applied this decoding method to an ECoG-based BMI system for real-time control of a robot arm (Fig. 2). We introduced successive SVM decoding every 200 ms. ECoGs were measured using a 128-channel digital EEG system (EEG 2000; Nihon Koden) and digitized at a sampling rate of 1000 Hz. The robot arm was an experimental anthropomorphic hand developed by Professor Yokoi [5]. The general movement mechanisms and degrees of freedom of the hand mimicked those of a human hand. The hand was equipped with eight DC motors to independently actuate eight individual tendons in the robot hand. The eight tendons work in a coordinated manner to accomplish flexion or extension of each individual finger. As a result, we succeeded in the voluntary control of the grasping and releasing of objects [6] (Fig. 3). Using a successive decoding and control algorithm, smooth robot hand movement was achieved even though the decoding accuracy on a single-trial basis was approximately 70%. We found that, in the case of paralyzed patients, just imagery of hand movement induces ECoG responses similar to those of real movements [3].

3. Fully Implantable Wireless System

Wired leads that penetrate the skin pose a high risk of infection. It is necessary to fully implant a recording system within the body in order to reduce infection risk through penetrating wire leads. For this reason, we are in the process of developing a fully implantable ECoG recording system (Fig. 4). This fully implantable system includes two 64-channel integrated analog amplifier chips, a Bluetooth wireless data transfer circuit and a wireless battery charger.

The integrated analog amplifier chip was designed for measuring ECoG Signals (Fig. 5). One chip functions with a 64-channel analog amplifier and 12-bit A/D converters at a maximum sampling rate of 1 kHz, and a size of 5.0 mm × 5.0 mm × 2.5 mm. In addition, this chip has a master/slave function so that two chips can deal with 128-channel signals. We adapted the Bluetooth protocol communication (Class 2) for the first prototype for high usability. A combination of two sets of Bluetooth circuits enabled effective data transmitting rates of 400 kbps. The wireless battery charging system consists of two parts — a transmitter outside the human body and a receiver inside the human body (abdominal part). We achieved a wireless

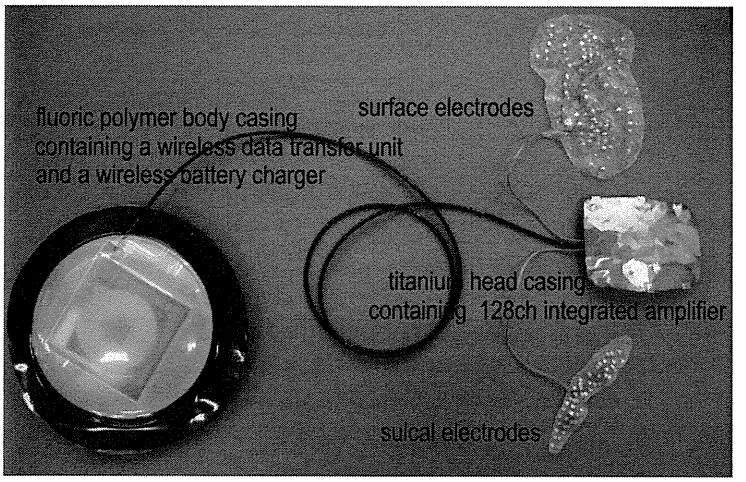

Figure 4. Prototype of a fully implantable ECoG recording system.

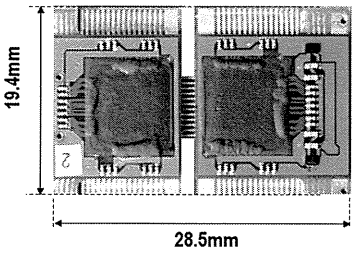

Figure 5. A 128-channel integrated analog amplifier system. This system includes two 64-channel analog amplifier chips on two small high-density mounting boards bridged by flexible wiring.

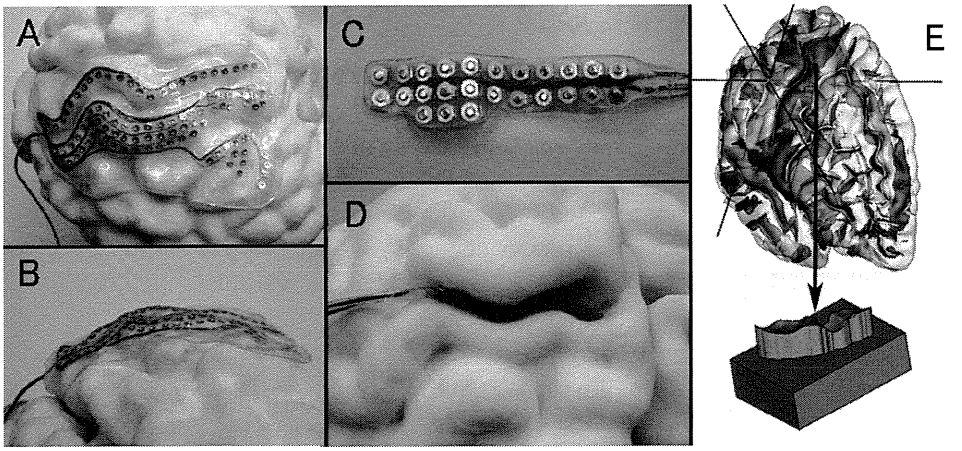

Figure 6. The 3-D high-density brain surface grid electrodes that fit individual brain surfaces. (A and B) Gyral (brain surface) electrodes. (C and D) Sulcal (brain groove) electrodes. (E) Mold designed with 3-D CAD software after automatic sulcal detection.

charging power of 4 W at a distance of 40 mm, which is sufficient to work the whole implantable system. The size of the abdominal part is 40 mm in diameter and 8 mm in thickness.

In addition, in order to record ECoGs with higher spatiotemporal resolution, we developed three-dimensional (3-D) high-density grid electrodes, which fit to an individual's brain surface [7]. We extracted 3-D surface data of the brain surface and the brain groove from the patient's individual magnetic resonance images. Automatic brain groove extraction software was used. Then we designed male and female molds for the grid electrodes using 3-D CAD software (Mimics; Materialize Japan) (Fig. 6). The molds were then rapidly produced by a 3-D printer. These 3-D grid electrodes fit to the brain surface with only minimal compression of the brain tissue and provide high ECoGs yields due to their close contact with the brain.

We developed a head casing made of titanium, which was cut to fit a patient's individual skull bone shape using 3-D CAD (Mimics) and 3-D CAM (Gibbs CAM; Gibbs and Associates) software (Fig. 7) [8]. This head casing not only has cosmetic advantages, but it is also safer because other convex shapes pose a higher risk of cutaneous fistula.

At this stage, we have developed the first prototype of a fully implantable system and have just started animal experiments. Further animal experiments will be needed before applying the implantable system to human clinical trials.

4. Importance of Neuroethics

Brain signals are the ultimate form of personal information, because they might include personal thoughts and emotions that subjects might not want others to know about. BMI research may allow us to decode such types of personal neural infor-

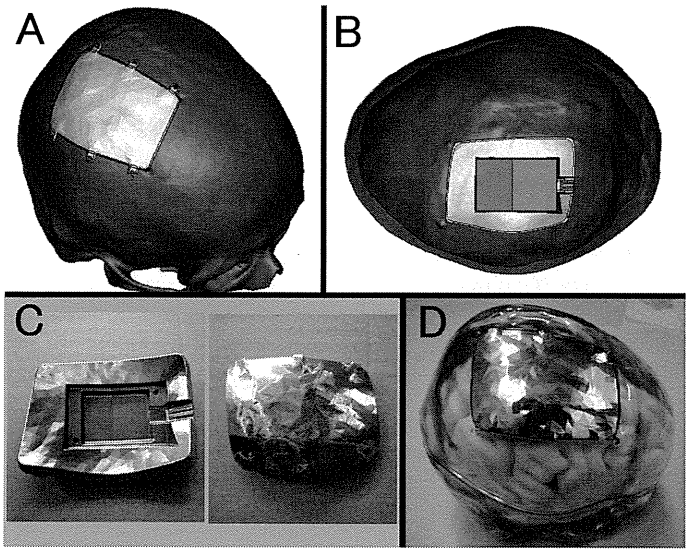

Figure 7. Titanium head casing fitted to a model of an individual's skull bone. (A and B) Head casing design using 3-D CAD. The 3-D skull bone data were obtained from an individual's computer tomography images. (A) Outer side view. (B) Inner side view. The head casing contains two 64-channel integrated amplifier chips on a small mounting board that are mounted on a folded inner panel as indicated. (C) Prototype casing. Left: inner side view. Right: outer side view. (D) Prototype casing placed on the skull and brain model made from individual magnetic resonance images.

mation. In addition, the effects of the BMI on brain function are still not completely known. Thus, the BMI arouses new ethical issues, known as neuroethics. We are addressing these ethical issues using an ethical consultation system that was set up within our research project.

5. Conclusions

We have developed an ECoG-based real-time BMI system and the first prototype of a fully implantable wireless system. The ECoG-based real-time BMI system successfully provided voluntary control over the grasping and opening of a robot hand. A fully implantable wireless system is indispensable for the clinical application of an invasive BMI to reduce the risk of infection.

Acknowledgement

This work was supported by the Strategic Research Program for Brain Sciences of MEXT.

References

1. J. R. Wolpaw, N. Birbaumer, D. J. Mcfarland, G. Pfurtscheller and T. M. Vaughan, Brain–computer interfaces for communication and control, *Clin. Neurophysiol.* **113**, 767–791 (2002).

2. Y. Kamitani and F. Tong, Decoding the visual and subjective contents of the human brain, *Nat. Neurosci.* **8**, 679–685 (2005).
3. T. Yanagisawa, M. Hirata, Y. Saitoh, A. Kato, D. Shibuya, Y. Kamitani and T. Yoshimine, Neural decoding using gyral and intrasulcal electrocorticograms, *Neuroimage* **45**, 1099–1106 (2009).
4. J. A. Rathelot and P. L. Strick, Subdivisions of primary motor cortex based on cortico-motoneuronal cells, *Proc. Natl. Acad. Sci. USA* **106**, 918–923 (2009).
5. H. Yokoi, K. Kita and T. Nakamura, Mutually adaptable EMG devices for prosthetic hand, *Int. J. Factory Automat. Robotics Soft Comput.*, 74–83 (2009).
6. T. Yanagisawa, M. Hirata, Y. Saitoh, T. Goto, H. Kishima, R. Fukuma, H. Yokoi, Y. Kamitani and T. Yoshimine, Real-time control of a prosthetic hand using human electrocorticograms, *J. Neurosurg.* **114**, 1715–1722 (2011).
7. M. Hirata, T. Yoshimine, Y. Saitoh, T. Yanagisawa, T. Goto, Y. Watanabe and T. Saito, Osaka University, Intracranial electrode and method for producing same, US patent application, 12/378,695 (2009).
8. M. Hirata, T. Yoshimine, K. Matsushita, T. Goto, T. Yanagisawa, T. Suzuki and S. Yoshimoto, Osaka University *et al.*, PCT patent application, PCT/JP2011/001402 (2011).

About the Authors

Masayuki Hirata, BS, MS, MD and PhD graduated from the Faculty of Engineering, University of Tokyo, in 1985, and Osaka University Medical School, in 1994. He is a board-certified neurosurgeon specialized in functional neurosurgery. He was promoted to a Specially-Appointed Associate Professor, Department of Neurosurgery, Osaka University Medical School, serving as a Leader of the Neural Engineering Group.

Kojiro Matsushita, BS and PhD, graduated from the Department of Engineering, Tokyo University of Science, in 2000, was a Research Fellow in the Department of Informatics, University of Zurich, in 2001–2002, Graduate Student in the Department of Informatics, University of Sussex, in 2003–2004, graduated from the Graduate School of Engineering, University of Tokyo, in 2007, and was a Postdoctoral Fellow in Computer Science and Artificial Intelligence Laboratory, MIT, in 2008. He was recruited as a Specially-Appointed Assistant Professor, Department of Neurosurgery, Osaka University Medical School, in 2009.

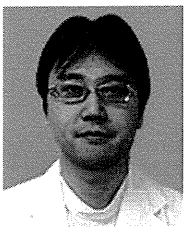

Takufumi Yanagisawa MD and PhD, graduated from Department of Physics, Waseda University and Osaka University Medical School, in 2005. He is a board-certified neurosurgeon. He learned decoding of brain signals under Kamitani Labo at ATR Computational Neuroscience Laboratories. He is currently appointed as a Specially-Appointed Researcher, Department of Neurosurgery, Osaka University Medical School with a principal interest in the decoding of eletrocorticograms.

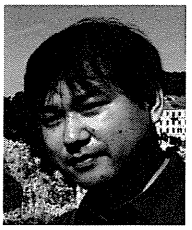

Tetsu Goto, MD and PhD, graduated from Osaka University Medical School, in 2002. He is a board-certified neurosurgeon, currently Assistant Professor, Department of Neurosurgery, Osaka University Medical School and Division of Health Sciences. He is specialized in the analysis of motor and language signals recorded with magneto-encephalography and electrocorticography.

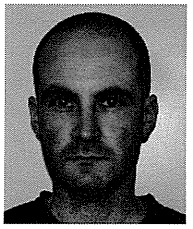

Shayne Morris received an MBA from Yokohama National University, in 1994. Following this he received an MD degree in Medicine from Osaka University, in 2002, and is presently in a PhD course at Osaka University, studying functional neurosurgery in Osaka University Graduate School of Medicine.

Hiroshi Yokoi received the BE, ME and PhD degrees in Engineering from Hokkaido University, in 1986, 1990 and 1993, respectively. From 1995, he was an Associate Professor at Hokkaido University. From 2004, he was an Associate Professor at the University of Tokyo. From 2009, he has been a Professor at the University of Electro-Communications.

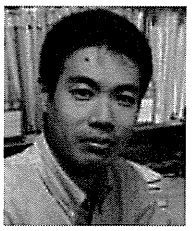

Takafumi Suzuki received the BE, ME and PhD degrees in Engineering from the University of Tokyo, in 1993, 1995 and 1998, respectively. From 1998 to 2002, he was a Research Associate at the University of Tokyo. He is currently an Assistant Professor at the Graduate School of Information Science and Technology, University of Tokyo.

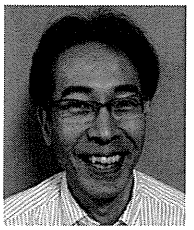

Takeshi Yoshida received the BE, ME and PhD degrees in Engineering from Hiroshima University, in 1994, 1996 and 2004, respectively. From 1996 to 2001, he was with System Electronics Laboratories, Nippon Telegraph and Telephone Corp. He is currently an Assistant Professor at the Graduate School of Advanced Sciences of Matter, Hiroshima University.

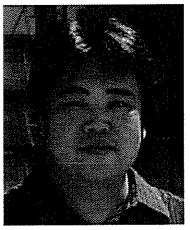

Fumihiro Sato received the BS and PhD degrees in Engineering from Tohoku Gakuin University, in 1995 and 2000, respectively. From 2000 to 2006, he was an Assistant Professor at Tohoku University. He is currently an Associate Professor of the Department of Electric Engineering, Tohoku University.

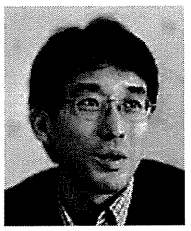

Osamu Sakura received the PhD in Science from Kyoto University, in 1990. From 1995 to 1999, he was an Associate Professor at the Faculty of Business Administration at Yokohama National University. From 2000 to 2006, he was an Associate Professor and, from 2007, he has been a Professor at the Graduate School of Interdisciplinary Information Studies, University of Tokyo.

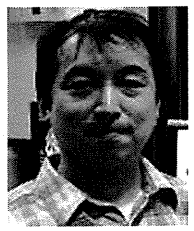

Yukiyasu Kamitani, PhD graduated from the University of Tokyo, in 1993, and received the PhD degree in Computation and Neural Systems from California Institute of Technology, in 2001. From 2001 to 2003, he was a Research Fellow at Beth Israel Deaconess Medical Center, Harvard Medical School. He moved to ATR Computational Neuroscience Laboratories, in 2004. After being a Senior Research Scientist, from 2007 to 2008, he is currently a Head of the Department of Neuroimformatics in the ATR Computational Neuroscience Laboratories.

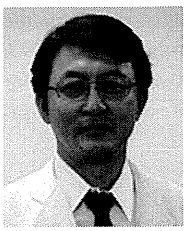

Toshiki Yoshimine, MD and PhD, graduated from Osaka University Medical School in 1975. He is a board-certified neurosurgeon, specialized in brain tumor and epilepsy surgery. He is a Director of the Japan Neurosurgical Society and Neurotrauma Committee Member, World Federation of Neurosurgical Societies. He has been a Research Fellow in the Mayo Clinic, in 1980–1983, and a Visiting Professor at the University of Mainz, in 1995. He currently serves as Professor and Chairman, Department of Neurosurgery, Osaka University Medical School and Director, Medical Center for Translational Research, Osaka University Hospital.